CrystEngComm

ROYAL SOCIETY OF CHEMISTRY

PAPER

View Article Online
View Journal | View Issue

Cite this: *CrystEngComm*, 2022, **24**, 7852

Crystal and molecular structure of series of triphilic ionic liquid-crystalline materials based on the 1,2,4-triazolium cation†

Alessio Riccobono, [ab] Adrian C. Whitwood, [a] Rachel R. Parker, [a] Sam Hart, [a] Andrea Pace, [b] John M. Slattery, [a] Ivana Pibiri *[b] and Duncan W. Bruce *[a]

Received 29th September 2022,
Accepted 20th October 2022

DOI: 10.1039/d2ce01354a

rsc.li/crystengcomm

Results from the determination of sixteen X-ray single crystal structures are reported for a series of 3-(4-alkoxyphenyl)-5-perfluoroalkyl-2,4-dimethyl-1,2,4-triazolium salts with tetrafluoroborate, triflate or bistriflimide anions, in which the lengths of the alkoxy and perfluoroalkyl chains are varied systematically. On account of these cations having a hydrocarbon, fluorocarbon and ionic part, they are classified as triphilic. All of the tetrafluoroborate salts crystallised in the $P2_1/c$ space group, most as acetone solvates, while for the bistriflimide salts, four different space groups were found although all contained a $P2_1$ screw axis often with additional symmetry elements. Of the triflates, two crystallised in space groups with a $P2_1$ screw axis and two in $P\bar{1}$. The organisation in the crystalline state tended to reflect the triphilic nature of the materials with cations and anions associating in repeating motifs, while the rest of the space was occupied by either hydrocarbon or fluorocarbon domains with only two exceptions.

Introduction

The different factors that drive the formation and organisation in liquid crystal mesophases are myriad. Considering calamitic materials, these relate, *inter alia*, to the nature of the (normally) rigid core (its length, volume, the presence or not of conjugation, polarity and its direction, steric factors) and the attached chains (nature, number, length, volume, position of attachment, chirality). One feature of interest is when a single mesogen contains both hydrocarbon and fluorocarbon chains, as their mutual immiscibility can have a profound influence on the molecular organisation in the mesophase and the material is formally amphiphilic.[1–9] For example, preference for self-association often leads to the formation of bilayer mesophases or, in some cases, to a change in the nature of the observed mesophase.[10]

An additional factor that can be brought to bear is the introduction of an ionic unit into the mesogen[11] and here, it is often observed that the resulting electrostatic self-association, with the concomitant exclusion of the aliphatic parts of the mesogen from the ionic domains, dominates self organisation so that the observation of lamellar phases, most usually SmA, normally prevails in calamitic systems.

Recently, we reported on the mesophase behaviour of some ionic liquid crystals (ILCs) that contained both hydrocarbon and fluorocarbon chains, leading to the idea of triphilic liquid crystals.[12,13] The structure of these salts, abbreviated as [TRYUM-*m*,*n*][X], is shown in Fig. 1 and briefly, their liquid-crystal properties can be summarised as follows:

- None of the salts with a perfluoropropyl chain (m = 3) was liquid crystalline.
- All of the liquid-crystalline salts showed a SmA phase and, in addition, the $[BF_4]^-$ salts showed a SmB phase at lower temperatures.
- The most stable mesophases were shown by the $[BF_4]^-$ salts, with clearing points in excess of 220 °C.

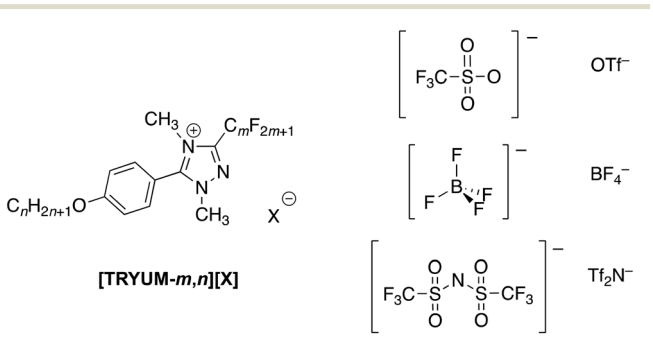

Fig. 1 Molecular structure of the salts in this study.

[a] Department of Chemistry, University of York, Heslington, York YO10 5DD, UK. E-mail: duncan.bruce@york.ac.uk; Tel: +44 (0)1904 324085
[b] Dipartimento di Scienze e Tecnologie Biologiche, Chimiche e Farmaceutiche, Viale delle Scienze, Ed. 1790128 Palermo, Italy. E-mail: ivana.pibiri@unipa.it

† Electronic supplementary information (ESI) available. CCDC 2177830–2177844. For ESI and crystallographic data in CIF or other electronic format see DOI: https://doi.org/10.1039/d2ce01354a

• The triflates showed the next most stable phases with clearing points above 150 °C, while the mesophases of the bistriflimide salts was lower again with many showing monotropic phases.

• The triflate and bistriflimide salts showed the lowest melting points, mostly between 60–100 °C, while those of the $[BF_4]^-$ salts were mostly above 100 °C.

The idea of triphilic ionic liquids (ILs) is not unique to this study and it has also been proposed to account for the liquid structure in mixtures of 1-methyl-3-alkylimidazolium bromides (Fig. 2a) in which the alkyl group is either C_8H_{17}– or $C_6F_{13}CH_2CH_2$–.[14]

An interesting feature of this study[14] and of our previous work[12] with the [TRYUM-*n*,*m*][X] salts is the appearance of a double reflection peak at small-angles in X-ray scattering experiments. This is observed in the isotropic phase of the liquid crystals (Fig. 2b) and of course in the simple mixture of the imidazolium ILs. In the mixture study, the observation was interpreted as evidence of a phase-separated, double domain (triphilic) structure,[14] whereas in the former example this is not possible (single-component system) and interpretation relied on local bilayer ordering.[12] That said, in reality the gross features of the organisation in both systems may actually be rather similar.

As part of the study of the triphilic ILCs and despite some of the chain lengths involved, which often frustrate crystallisation, we were successful in obtaining a significant number of X-ray single crystal structures and it became of interest to see the extent to which separation between hydrocarbon and fluorocarbon chains extended into solid-state organisation. Of course, it is well recognised that extrapolating solid-state organisation into predictions about LC mesophase organisation is not to be recommended. However, using data from solid, LC and liquid states may provide some additional understanding of these complex systems. As such, data from these crystal structure determinations are now presented and discussed.

Preparation and crystallisation

The salts were prepared as described previously.[12,13] In all cases, single crystals were obtained by first dissolving 10–15 mg of the material in acetone (enough to dissolve the material completely) in a glass tube and then adding hexane as antisolvent until the mixture became just cloudy. Sufficient additional drops of acetone were then added to give a clear solution after which this tube was placed in a larger tube containing antisolvent (hexane) and sealed. Single crystals tended to grow over 3–7 days as the more volatile (acetone) solvent evaporated, thus increasing the local concentration of antisolvent. Cif and Cifcheck files are found in the ESI.† Where the structure showed disorder, modified cif files have been created (not deposited) to allow the display of structures with the disorder removed for clarity. Modified cifs have also been used in some cases where there is solvent of crystallisation.

Data were collected at 110 K for all crystals except for [TRYUM-7,12][Tf_2N], [TRYUM-9,12][Tf_2N], [TRYUM-3,14][Tf_2N] and [TRYUM-9,14][Tf_2N], all of which demonstrated a change in crystal system on cooling that destroyed the single crystal. In these instances, data were collected at 220 K.

CCDC numbers for the salts are: 2177830–2177844. Data for [TRYUM-7,10][OTf] were published previously[13] (CCDC 1848982).

Results

The materials prepared are shown in Fig. 1, within which there are three variables – hydrocarbon chain length (n = 10, 12, 14), fluorocarbon chain length (m = 3, 7, 9) and anion (X = $[OTf]^-$, $[BF_4]^-$, $[Tf_2N]^-$). Varying these gave a matrix of twenty-seven materials. For the purposes of the structural study, comparisons were made as follows:

• Between nine salts in which the hydrocarbon chain length was held constant with n = 10 while m and X were varied.

• Two comparisons of three structures in which m and X are constant (m = 7, X = $[Tf_2N]^-$ and m = 9, X = $[Tf_2N]^-$).

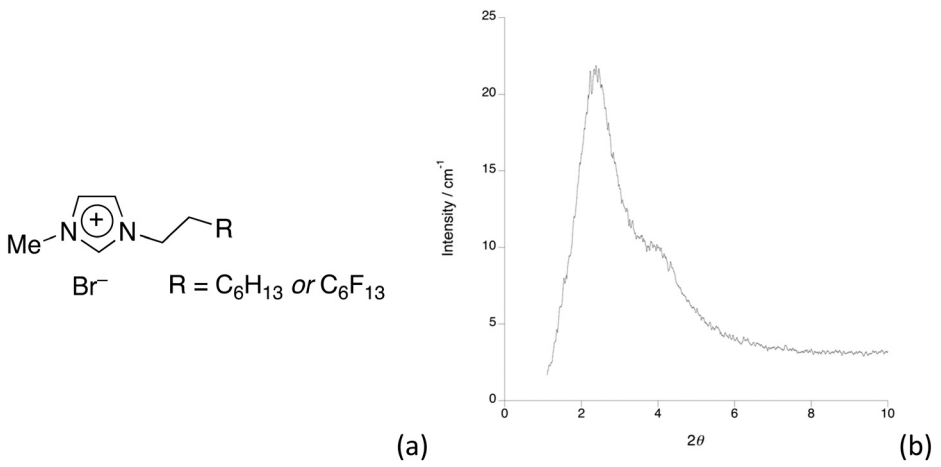

Fig. 2 (a) Imidazolium ILs used in mixture studies[6] and (b) SAXS pattern in the isotropic liquid phase of [TRYUM-7,10][Tf_2N] at 89 °C.[13]

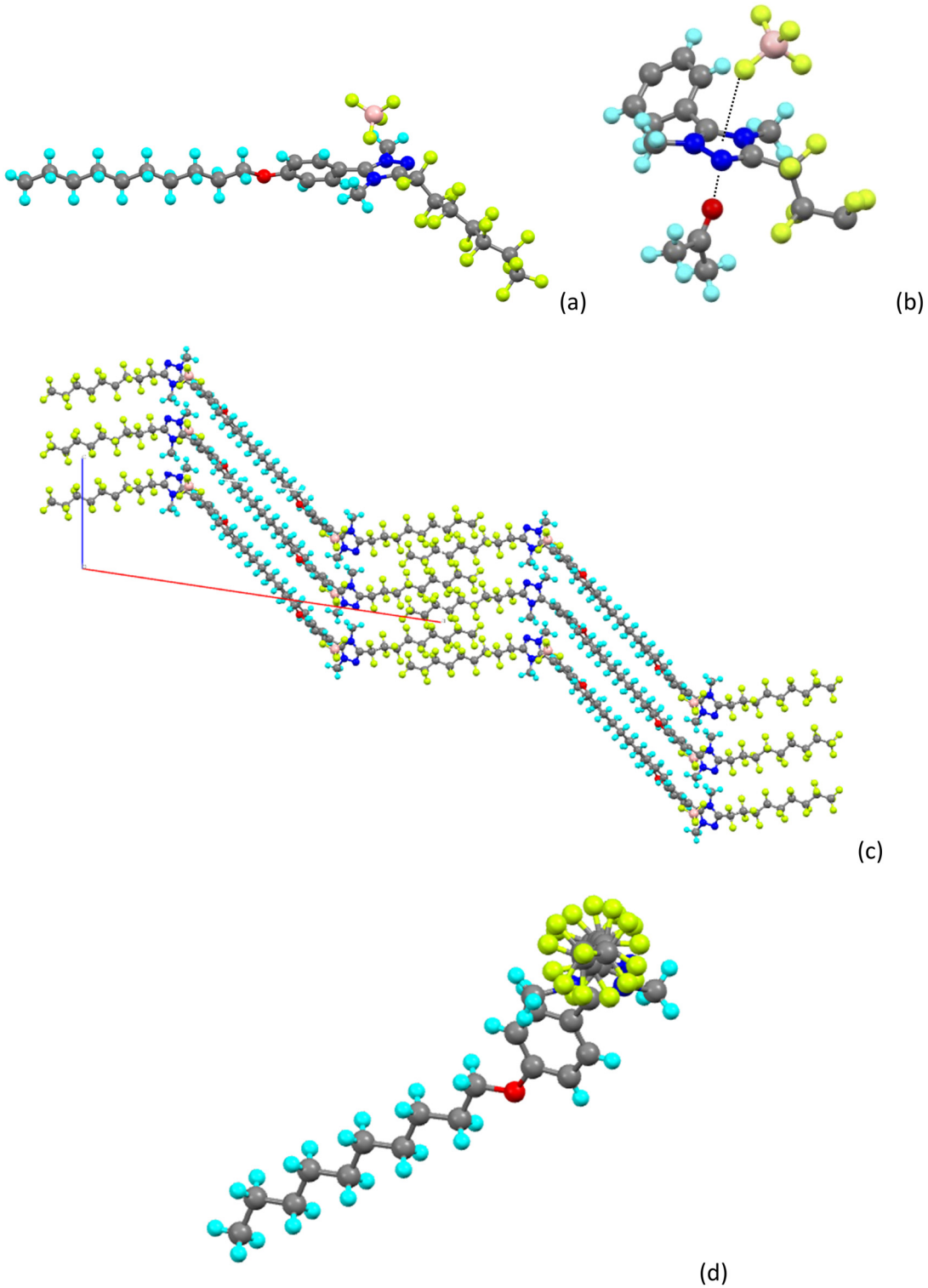

Fig. 3 Indicative structural motifs for the $[BF_4]^-$ salts: (a) the disposition of the cation and anion in [TRYUM-7,10][BF_4], (b) the local structure of the cation in [TRYUM-9,14][BF_4]·(acetone). Black dashed lines indicate anion/solvent to imidazolium ring centroid distances; (c) packing viewed down the *b* axis of [TRYUM-9,10][BF_4]; (d) view to show the helical nature of the fluorocarbon chain in [TRYUM-9,10][BF_4] – disorder and anion removed for clarity.

- A comparison of three structures where both *n* and *m* are constant (*n* = 14, *m* = 9) and X is varied (X = $[OTf]^-$, $[BF_4]^-$, $[Tf_2N]^-$).‡

‡ One other structure was determined – ([TRYUM-3,14][Tf_2N]) – and is reported in the ESI.

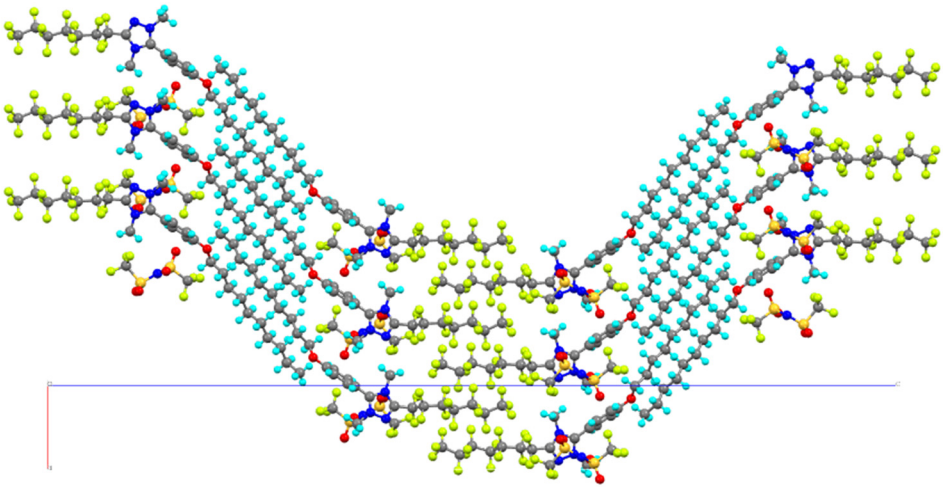

Fig. 4 Packing of [TRYUM-7,10][Tf_2N] viewed down the *b*-axis to show the extent of the *c*-axis (in blue).

Results and discussion

Tetrafluoroborate salts

All salts crystallised in the $P2_1/c$ space group with [TRYUM-3,10][BF_4], [TRYUM-9,10][BF_4] and [TRYUM-9,14][BF_4] being acetone solvates while [TRYUM-7,10][BF_4] was not. The *b*- and *c*- lattice parameters were very similar for all structures ($b \approx$ 9.2–9.4 Å; $c \approx$ 11.1–11.7 Å), whereas *a* varied with the length of the appended chains. For the acetone solvates, *a* increased from 29.5 to 37.1 Å as *m* increased from 3 to 9 and then increased from 37.1 to 40.3 Å as *n* increased from 10 to 14. Its value for [TRYUM-7,10][BF_4] (29.9 Å) was almost identical to that of [TRYUM-3,10][BF_4] (29.5 Å), which is accounted for by slightly tighter packing possible in the former in the absence of the acetone solvate.

As seen previously for 1,4,5-trimethyl-3-perfluorooctyl-1,2,4-triazolium tetrafluoroborate (Fig. S1†),[15] the triazolium cations were closely associated with the tetrafluoroborate anions (Fig. 3a) and for the solvates, the local structure around the cation shows the close approach of a fluorine from a $[BF_4]^-$ anion and the oxygen of an acetone (Fig. 3b). The distances between the cation ring centroid and the fluorine and oxygen are remarkably consistent in these solvates: *d*(centroid···F) = 2.933(1) Å, 2.926(3) Å and 2.937(2) and *d*(centroid···O) = 2.854(2) Å, 2.851(4) Å and 2.853(3) Å for [TRYUM-3,10][BF_4], [TRYUM-9,10][BF_4] and [TRYUM-9,14][BF_4], respectively. Interestingly, the *d*(centroid···F) distance (2.802(3) Å) is slightly shorter in unsolvated [TRYUM-7,10][BF_4], likely reflecting the different electrostatics with the close approach of a single electronegative atom. The structure of (unsolvated) [TRYUM-7,10][BF_4] then shows a $[BF_4]^-$ anion on one side of the triazolium ring, while on the other there are no close contacts and the space is occupied by the terminal fluorine atoms of interdigitated chains.

All of these salts showed an effectively identical packing motif with evident separation between the fluorocarbon and hydrocarbon chains and the structure propagates with interdigitation between the chains of the same type (Fig. 3c). Finally, for the three salts with $m = 7$ or 9, the structures show disorder of the fluorocarbon chains, which is associated with their helical nature as shown in Fig. 3d. Such helicity is a common feature of fluoroalkyl chains.

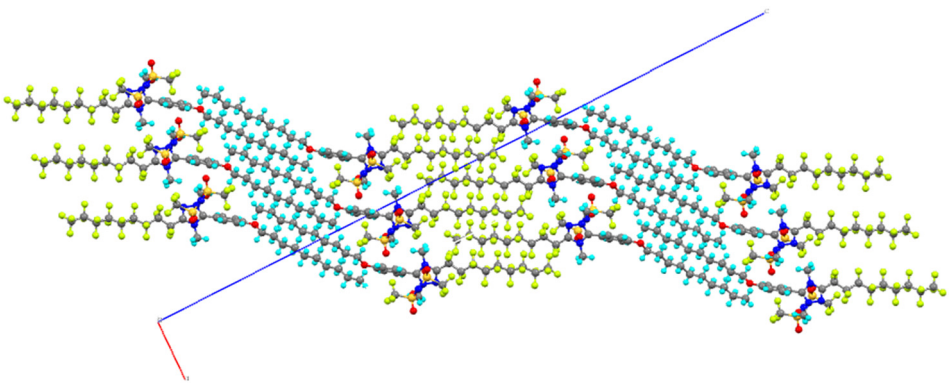

Fig. 5 Packing in [TRYUM-9,10][Tf_2N] viewed down the crystallographic *b*-axis.

Bistriflimide salts

This represents the largest group of structures studied, within which there are many common features. Four salts crystallise in the space group $P2_12_12_1$, two in $P2_1/c$ and one each in $P2_1/n$ and $P2_1$; none is a solvate. Despite the different space groups, the overall organisation for each salt is very similar, which is also reflected in the crystallographic parameters. Thus, the *a* and *b* lattice parameters are remarkably similar varying only between 6.70 and 6.84 Å for *a*, and between 8.46 and 8.66 Å for *b*. In contrast, the *c* parameter is large and scales with the length of both the hydrocarbon and the fluorocarbon chains. Thus, *c* changes from 56.35 to 71.56 Å as *m* increases from [TRYUM-3,10][Tf_2N] to [TRYUM-9,10][Tf_2N] and from 71.56 to 78.21 Å as *n* increases from [TRYUM-9,10][Tf_2N] to [TRYUM-9,14][Tf_2N]. Fig. 4 shows a view of [TRYUM-7,10][Tf_2N] down the *b*-axis with the extent of the *c*-axis indicated, showing how it scales with the length of the cation. The same figure also shows the way in which the salts pack, with separation between the hydrocarbon and fluorocarbon segments, each of which self-interdigitates with neighbouring cations to propagate the structure. In all of the structures, the longer fluorocarbon chains show their helical arrangement, although careful examination shows the beginnings of the helicity even in the perfluoropropyl chains.

This undulating motif is seen for [TRYUM-3,10][Tf_2N], [TRYUM-7,10][Tf_2N], [TRYUM-7,12][Tf_2N], [TRYUM-3,14][Tf_2N] and [TRYUM-7,14][Tf_2N], whereas a more zig-zag packing is seen for [TRYUM-9,10][Tf_2N], [TRYUM-9,12][Tf_2N] and [TRYUM-9,14][Tf_2N] (Fig. 5). Interestingly and perhaps coincidentally, these last three all have a perfluorononyl chain.

A point of difference with the $[BF_4]^-$ salts is that in all of the bistriflimides, there are cation···anion interactions that perpetuate along the crystallographic *b*-axis, with the closest approach being between the triazolium ring and a sulfonyl oxygen from the anion. The unsymmetric arrangement (O···centroid = 2.987(3) Å and 3.190(3) Å), which is shown in Fig. 6, involves two oxygen atoms of the same sulfonyl group bridging two of the heterocyclic rings.

The unit cell of [TRYUM-3,14][Tf_2N] contains two independent cations, which differ in the way the perfluoropropyl chain is disposed with respect to the triazolium ring (see also below). Thus, in one it begins to propagate perpendicular to the plane of the heterocyclic ring (Fig. 6a), while in the other it propagates in the plane of the ring (Fig. 6b). A quick examination of several other structures in this study shows both types of arrangement to occur.

Triflate salts

Of the four salts studied, two crystallised in the $P\bar{1}$ space group, one in $P2_1/n$ and the other in $P2_1/c$. There was much less uniformity in the unit cell dimensions among these salts, although all showed an extended *c*-axis (from 20.8 to 39.4 Å). Indeed, these salts show the greatest diversity of molecular arrangement and as such, each is described separately.

For [TRYUM-3,10][OTf], the diffraction from the crystal was weak and smeared in certain directions, presumably due to slippage of layers leading to a much less well resolved structure (R_1 = 11.3%). There are two cation-anion pairs in the unit cell and both of the decyl chains were disordered, while one terminal perfluoropropyl chain was modelled in two positions with refined occupancies of about 3 : 1 (Fig. 7). For the other, the six terminal carbon atoms were modelled in two positions with refined occupancies of 0.723 : 0.277(8). For the disordered chains, the C–C bond lengths were restrained to be 1.52 Å and the C–C–C distances restrained to be 2.48 Å. The two cations in the unit cell differed in their alkyl chains with a gauche C–C–C bond at C_2 in one chain (cation 1) and at C_7 in the other (cation 2).

Each cation is 'sandwiched' between two triflate anions with unsymmetric centroid···oxygen atom separations: O···centroid 2.836(6) and 2.974(6) Å (cation 1), and O···centroid 2.826(6) and 3.006(6) Å (cation 2). The structure

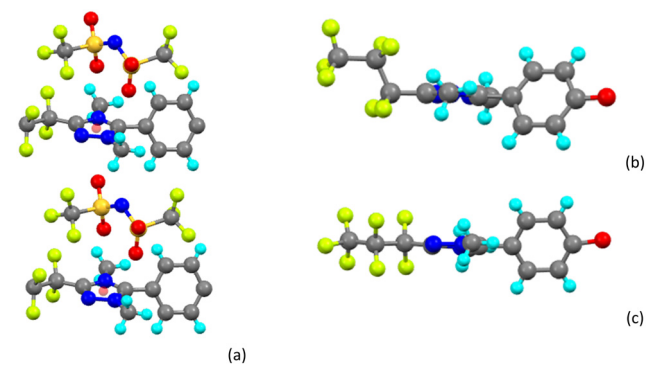

Fig. 6 (a) Cation···anion stacking in [TRYUM-9,10][Tf_2N] (cations truncated for clarity); (b and c) side-on views of a portion of the cation of [TRYUM-3,14][Tf_2N] showing the different arrangements of the perfluoropropyl chain with respect to the triazolium ring.

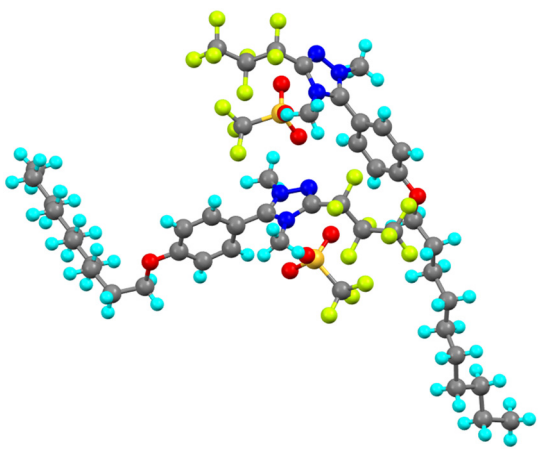

Fig. 7 The two independent cation-anion pairs in the unit cell of [TRYUM-3,10][OTf].

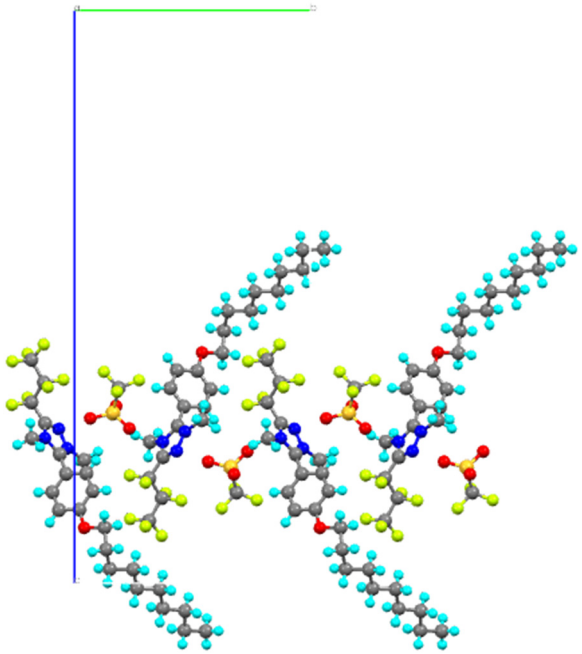

Fig. 8 Propagation of cation 1 of [TRYUM-3,10][OTf] viewed down the crystallographic *a*-axis.

propagates as a second atom on each triflate anion bridges to another triazolium cation and each 'chain' so formed contains exclusively cation 1 or cation 2. Fig. 8 shows this for

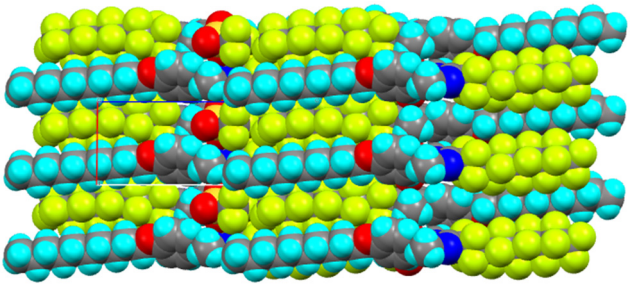

Fig. 10 Views of the structure and packing of [TRYUM-9,10][OTf] viewed down the *b*-axis. Projection along the *a*- and *c*-axes are found as Fig. S2.†

cation 1, while Fig. S2a† shows the arrangement for cation 2 and Fig. S2b† shows an illustration of how the two propagating structures interrelate.

[TRYUM-7,10][OTf] has been reported previously,[13] but further analysis has revealed additional detail not contained in the earlier publication. The salt crystallises in the $P2_1/c$ space group and, in common with the triflimides, shows cation···anion stacking along the *b*-direction. Two triflates are almost superimposed on either side of the triazolium ring with O···centroid distances of 2.934(7) and 3.066(2) Å, with each triflate bridging two triazolium rings. This is seen in Fig. 9a, which also shows a view of the propagation when viewed down the crystallographic *c*-axis with the expected

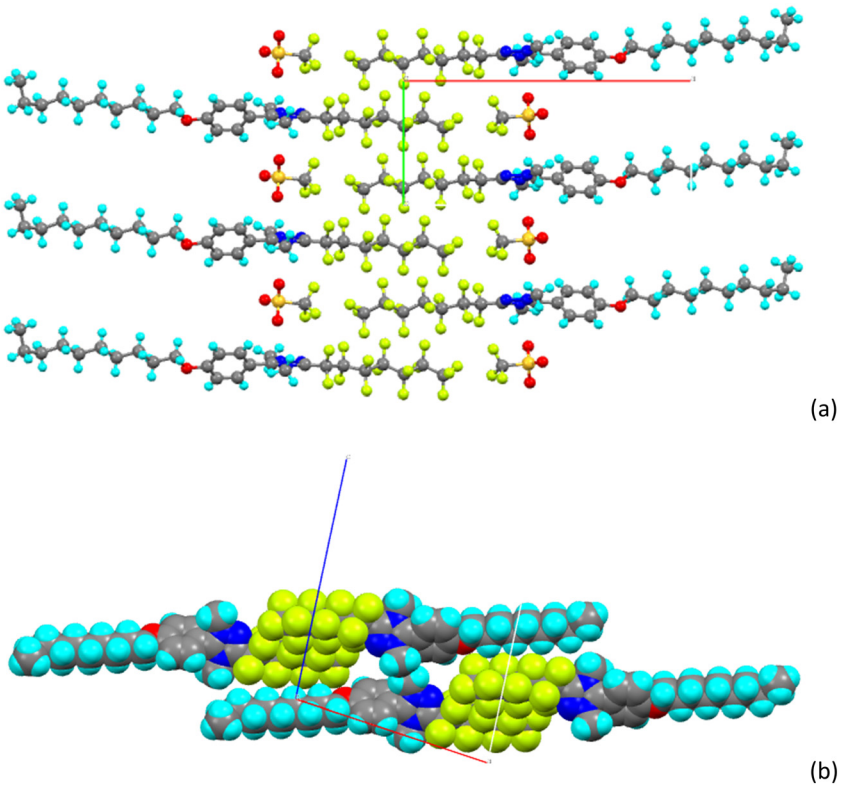

Fig. 9 Aspects of the packing in [TRYUM-7,10][OTf] showing (a) cation…anion stacking and the segregation of hydrocarbon and fluorocarbon chains viewed down the *c*-axis and (b) the interaction between hydrocarbon and fluorocarbon chains viewed down the *b*-axis (anions omitted for clarity).

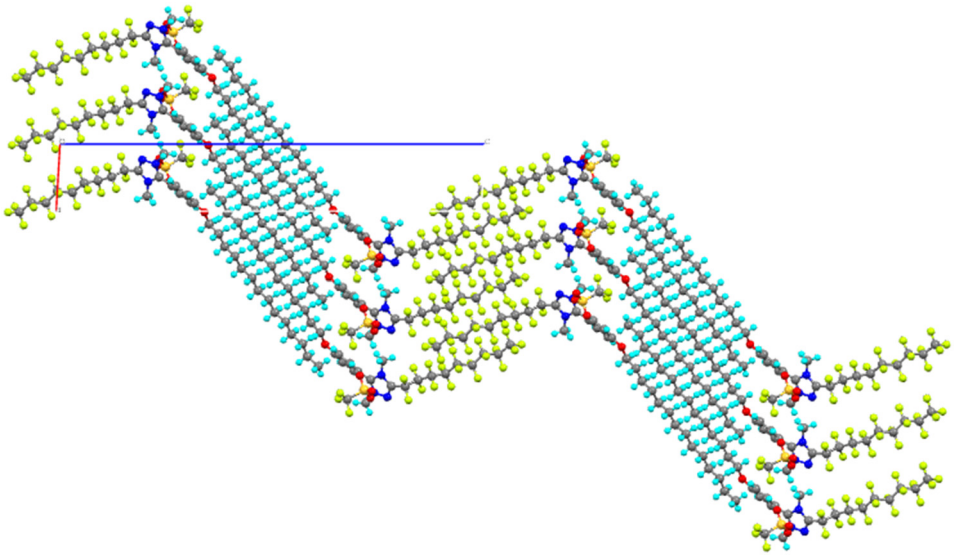

Fig. 11 Molecular structure of [TRYUM-9,14][OTf] viewed down the crystallographic *b*-axis showing the propagation of the structure.

segregation of the fluorocarbon and hydrocarbon regions. However, if the packing is extended further, then viewed down the *b*-axis in space-filling presentation (Fig. 9b), it is seen that the propagating unit is shifted along the *a*-axis in such a way that the hydrocarbon and fluorocarbon regions overlap with one another. In the fluorocarbon regions, the shortest F···F separation is 2.840(3) Å, while in the 'mixed' region, the shortest H···F separation is 2.634(2) Å. Considering the reported van der Waals radii of 1.20 Å (H) and 1.46 Å (F), then these are just at the limits of what might be considered as overlap. Thus, while attractive H···F interactions may contribute to the formation of the observed structure, if they do then it appears that they do so only rather weakly.

[TRYUM-9,10][OTf] crystallises in the $P\bar{1}$ space group and, in a manner directly analogous with [TRYUM-7,10][OTf], shows cation···anion stacking in the crystallographic *a*-direction with O···centroid distances of 2.807(6) and 2.932(9) Å. The structure contains disorder as described in the cif file and, in common with [TRYUM-9,14][OTf], there is disorder of the fluorocarbon chains but without helicity (see below).

Growing the structure initially shows a segregated structure akin to that found in [TRYUM-7,10][OTf], but it quickly becomes apparent that, once more, there is overlap between hydrocarbon and fluorocarbon regions, which shows up well in projections along the three axes (Fig. 10 and S3†). This time, the closest F···F separation is 2.786(4) Å, while the closest H···F separation is 2.567(2) Å, both shorter than those in [TRYUM-7,10][OTf].

[TRYUM-9,14][OTf] crystallises in the $P\bar{1}$ space group as an acetone solvate and, in a manner similar to that found for the $[BF_4]^-$ salts, there was close approach (Fig. S4†) of an acetone oxygen to one face of the triazolium ring (O···centroid = 2.752(5) Å) and of a triflate oxygen to the other (O···centroid = 2.849(6) Å). The structure propagates through overlap/interdigitation of hydrocarbon chains with hydrocarbon chains and fluorocarbon chains with fluorocarbon chains as shown in Fig. 11. This is viewed down the *b*-axis and the long (39.42 Å) *c*-axis is left-to-right in the plane of the page. An interesting feature of these salts is that the fluorocarbon chains do not exist in a simple helical arrangement, which may be a consequence of the packing of the chains where they overlap (Fig. S5†).

Discussion

The structure of all of these salts is dominated by electrostatic interactions between the cation and anion and this polar region is bounded by a hydrocarbon-rich area to one side and a fluorocarbon-rich area to the other. In all but two cases (see below), these regions are fully segregated. However, an interesting point to note is that in all of the discussions above, the 'cation···anion' interactions have been characterised and discussed as between the centroid of the

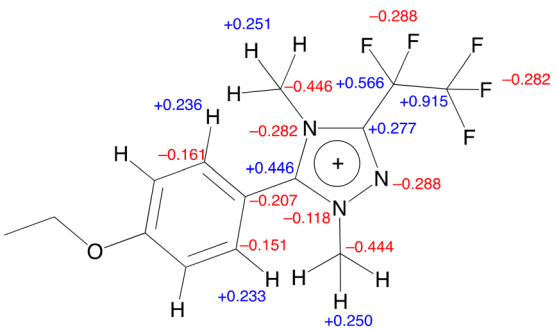

Fig. 12 Gas-phase NBO calculations of partial charges for a model cation at the PBE0/def2-TZVPP//BP86/SV(P) level of theory, showing partial charges for representative atoms around the triazolium core are shown. Where groups are expected to be freely rotating (*e.g.* CH_3) the average partial charge for the equivalent atoms is shown.

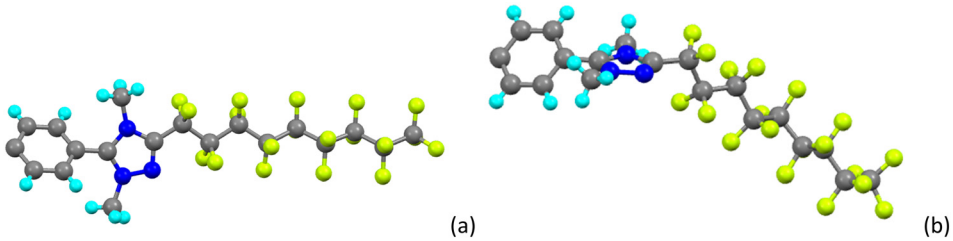

Fig. 13 Central part of the cations of (a) [TRYUM-9,10][OTf] and (b) [TRYUM-9,14][OTf] showing the different propagation of the perfluorocarbon chains from the triazolium ring.

triazolium ring and an oxygen of $[OTf]^-$ or $[Tf_2N]^-$, or the fluorine of $[BF_4]^-$, with additional note taken of interactions with solvent acetone where it is present. In order to explore this further, natural bond orbital (NBO) partial charges were calculated for a simplified cation at the PBE0/def2-TZVPP//BP86/SV(P) level (Fig. 12; full method description in the ESI†). These show that the positive charge on the cation is highly delocalised across the ring and peripheral groups. There is a relatively small residual positive charge of +0.15 on the ring, if the partial charges on the five ring atoms are summed, with positive partial charges localised on the two ring carbons and negative partial charges on nitrogen atoms, consistent with their relative electronegativities. No attempt has been made to deconvolute the different distances between anion (or solvent) 'donor' atoms and the different ring atoms, not least as the shortest distance is often to one of the (negatively charged) ring nitrogen atoms and it is for that reason that distance to ring centroid has been discussed above. Interestingly, there is also significant positive charge on the hydrogen atoms of the ring-bound methyl groups, yet there is no indication of hydrogen bonding to any anion from these C–H bonds.

However, searching within the Cambridge database shows that such interactions between an anion and the face of a cation are less common in 1,3-dialkylimidazolium systems (Fig. S6†), where anion···hydrogen interactions tend to dominate, although interestingly, analysis using the Mercury software package does not show them as hydrogen-bonded (see ESI†).

With the exception of [TRYUM-3,10][OTf], where there are two cation types in the unit cell (one with a gauche C–C–C link close to the ionic core and the other with a gauche link towards the end of the hydrocarbon chain), cation stereochemistry is of one of two types. Thus for all of the $[BF_4]^-$ salts, for [TRYUM-9,14][OTf] and all of the $[Tf_2N]^-$ salts except [TRYUM-9,14][Tf_2N], [TRYUM-9,12][Tf_2N] and [TRYUM-9,10][Tf_2N] and [TRYUM-3,10][Tf_2N], the cation is angled about the triazolium ring. This occurs by virtue of the fluorocarbon chain propagating perpendicular to the plane of the heterocyclic ring and, for example, the angle at the centroid of the triazolium ring made by considering the distant *ipso*-carbon of the phenyl ring and the terminal carbon of the fluorocarbon chain is 126.31(7)° for [TRYUM-9,14][OTf]. In contrast, for the remaining cations, *viz* [TRYUM-9,10][OTf] plus the bistriflimide salts just listed, the perfluorocarbon chain propagates co-planar with the triazolium ring and the same angle at the triazolium centroid for [TRYUM-9,10][OTf] is 170.59(4)°. Fig. 13 shows a small section of the two cations used for these measurements.

There is no correlation between the relative chain disposition in the cations and the mode of packing, but it is noteworthy that the undulating motif (Fig. 4) is seen only in bistriflimide salts. It is also true that, with one exception ([TRYUM-9,10][OTf]), all salts with a C_9H_{19}– hydrocarbon chain adopt a more zig-zag packing motif, but it is difficult to see how cause and effect may originate.

In both series of salts with oxygen-containing anions, the anions bridge pairs of cations, the one exception being [TRYUM-9,14][OTf] which crystallises as an acetone solvate and so mimics the $[BF_4]^-$ salts in having an anion on one side of each triazolium ring and an acetone on the other.

As might have been predicted, the mutual incompatibility of hydrocarbon and fluorocarbon chains is seen in all of these structures with the exception of [TRYUM-7,10][OTf] and [TRYUM-9,10][OTf]. This is perhaps somewhat surprising given the quite long perfluorocarbon chains in these two salts, but clearly the driving force for separation is readily overcome by the other terms in the lattice energy. The fact that the melting points of these salts are in line with what would be expected also suggests that the relative disposition of the two types of chain does not affect the stability of the crystal.

Author contributions

AR prepared the materials and grew the crystals used in the study; ACW, RRP and SH collected crystallographic data, and solved and refined the structures; JMS performed the computational work; DWB wrote the manuscript and prepared the drawings, both of which were commented on by IP and JMS; DWB, JMS, IP and AP conceptualised the study, supervised the work and secured the funding.

Conflicts of interest

The authors declare no conflicts of interest.

Acknowledgements

AR and RRP thank the University of York for support. AR also thanks the Università degli Studi di Palermo for support.

References

1 F. Guittard, E. Taffin de Givenchy, S. Geribaldi and A. Cambon, *J. Fluorine Chem.*, 1999, **100**, 85–96.
2 C. Tschierske, *Top. Curr. Chem.*, 2012, **318**, 1–108; M. Hird, *Chem. Soc. Rev.*, 2007, **36**, 2070–2095.
3 F. Lo Celso, I. Pibiri, A. Triolo, R. Triolo, A. Pace, S. Buscemi and N. Vivona, *J. Mater. Chem.*, 2007, **17**, 1201–1208.
4 A. Abate, A. Petrozza, G. Cavallo, G. Lanzani, F. Matteucci, D. W. Bruce, N. Houbenov, P. Metrangolo and G. Resnati, *J. Mater. Chem. A*, 2013, **1**, 6572–6578.
5 I. Zama, G. Gorni, V. Borzatta, M. C. Cassani, C. Crupi and G. Di Marco, *J. Mol. Liq.*, 2016, **223**, 749–753.
6 G. Cavallo, G. Terraneo, A. Monfredini, M. Saccone, A. Priimagi, T. Pilati, G. Resnati, P. Metrangolo and D. W. Bruce, *Angew. Chem., Int. Ed.*, 2016, **55**, 6300–6304.
7 S. Pensec, F.-G. Tournilhac, P. Bassoul and C. Durliat, *J. Phys. Chem. B*, 1998, **102**, 52–60.
8 V. Percec, G. Johansson, G. Ungar and J. Zhou, *J. Am. Chem. Soc.*, 1996, **118**, 9855–9866.
9 A. Schaz, E. Valaityte and G. Lattermann, *Liq. Cryst.*, 2004, **31**, 1311–1321.
10 A. Gainar, M.-C. Tzeng, B. Heinrich, B. Donnio and D. W. Bruce, *J. Phys. Chem. B*, 2017, **121**, 8817–8828.
11 K. Goossens, K. Lava, C. W. Bielawski and K. Binnemans, *Chem. Rev.*, 2016, **116**, 4643–4807.
12 A. Riccobono, G. Lazzara, I. Pibiri, A. Pace, J. M. Slattery and D. W. Bruce, *J. Mol. Liq.*, 2021, **321**, 114758.
13 A. Riccobono, R. R. Parker, A. C. Whitwood, J. M. Slattery, D. W. Bruce, I. Pibiri and A. Pace, *Chem. Commun.*, 2018, **54**, 9965–9968.
14 O. Hollůczki, M. Macchiagodena, H. Weber, M. Thomas, M. Brehm, A. Stark, O. Russina, A. Triolo and B. Kirchner, *ChemPhysChem*, 2015, **16**, 3325–3333.
15 H. Xue, B. Twamley and J. M. Shreeve, *J. Org. Chem.*, 2004, **69**, 1397–1400.